Spontaneous persistent currents in magnetically ordered graphene ribbons

D. Soriano (1,2), J. Fernández-Rossier (1)
(1) Departamento de Fìsica Aplicada, Universidad de Alicante, San Vicente del Raspeig, Spain
(2) Instituto de Ciencia de Materiales de Madrid, CSIC, Cantoblanco E28049, Madrid, Spain
(Dated: March 31, 2010)

We present a new mechanism for dissipationless persistent charge current. Two dimensional topological insulators hold dissipationless spin currents in their edges so that, for a given spin orientation, a net charge current flows which is exactly compensated by the counter-flow of the opposite spin. Here we show that ferromagnetic order in the edge upgrades the spin currents into persistent charge currents, without applied fields. For that matter, we study an interacting graphene zigzag ribbon with spin-orbit coupling. We find three electronic phases with magnetic edges that carry currents reaching 0.4nA, comparable to persistent currents in metallic rings, for the small spin orbit coupling in graphene. One of the phases is a valley half-metal.

PACS numbers:

Ordered electronic phases can emerge in condensed matter with properties fundamentally different from those of the constituent atoms. Two main different scenarios are known that result in the emergence of nontrivial electronic order. On one side, spontaneous symmetry breaking driven by many-body interactions which accounts for the existence of the crystalline order in solids and the variety of ordered electronic phases they can present, like superconductivity and ferromagnetism [1]. On the other side, topological order, which accounts for the robust quantized properties of the electron gas in the Quantum Hall regimes, and, more recently, on the properties of the so called topological insulators[2–5]. Whereas Integer Quantum Hall state is driven by an external magnetic field, topological insulators are driven by spin orbit interaction. They are different from conventional insulators because of their conducting surface (or edge) spin states which can be either chiral or spin-filtered and are robust with respect to time-reversal symmetric perturbations [2–6].

The experimental finding of topological insulators[7, 8] and their exotic surface (edge) states, motivates the general questions of whether and how electronic interactions could produce electronic phase transitions in the surface or edge states of a topological insulator, and what would be the consequences of such symmetry breaking. Here we address these questions in the case of a graphene ribbon with zigzag edges, a system that atracts enormous interest [3, 4, 9–22] in the context of spintronics[3, 4], magnetoelectronics[10, 12, 13, 17, 18, 20, 22] and valleytronics[16] . When described with a one orbital tight-binding model, graphene zigzag ribbons are conducting because of two degenerate almost flat bands associated to states localized at the edges [9]. Importantly, the zigzag states preserve the valley character [11, 16] of two dimensional graphene. When considered separately, the effect of electronic repulsion and spin orbit interactions over the system is dramatic and has been widely studied. On one side, it was soon recognized that electron Coulomb repulsion, in the Hubbard model, results in ferromagnetic order at the edges of the ribbon [10]. In the ground state the edges are counter-polarized and according to both density functional calculations [12] and to mean field Hubbard model[20], a gap opens so that the ribbon is an antiferromagnetic insulator.

When Coulomb repulsion is neglected, spin orbit (SO) interaction opens a gap in the spectrum of bulk graphene[23, 24] which is accompained by the emergence of spin filtered edge states at the Fermi energy[3, 4]. These two features, a spin-orbit driven gap and the emergence of topologically robust edge states, are the main properties of Topological Insulators[2–6]. Thus, the Coulomb driven and the SO driven phase have very different magnetic and conducting properties. Here we address the electronic properties of the ribbon when both Coulomb repulsion and spin orbit coupling are considered within a mean field Hubbard model[10, 20] with Kane-Mele spin orbit coupling[3, 4]. We report two main findings. First, in the presence of SO coupling the states with counter-polarized ferromagnetic edges break valley symmetry and, above a critical SO strength, the gap closes in one valley only, resulting in a valley half-metal. Second, in the presence of SO coupling ferromagnetic edges give rise to charge currents in the edges without an applied magnetic field.

We consider the one orbital Hubbard model in a honeycomb zigzag ribbon, at half filling, with the addition of the Kane-Mele SO coupling[3]:

$$\mathcal{H} = \sum_{i,j,\sigma} t_{i,j}(\sigma) c^{\dagger}_{i,\sigma} c_{j,\sigma} + U \sum_{i} n_{i\uparrow} n_{i\downarrow} \qquad (1)$$

The hopping matrix $t_{ij}(\sigma)$ in the first term accounts both for the standard first-neighbor spin-independent hopping t and the Kane-Mele-Haldane (KMH) second neighbor spin-orbit coupling[3, 4, 25]. The amplitude of the latter is given by the expression $it_{KM}\sigma\hat{z}\cdot\left(\vec{d}_1\times\vec{d}_2\right)$, where $\vec{d}_{1,2}$ are unit vectors along the direction of the bond

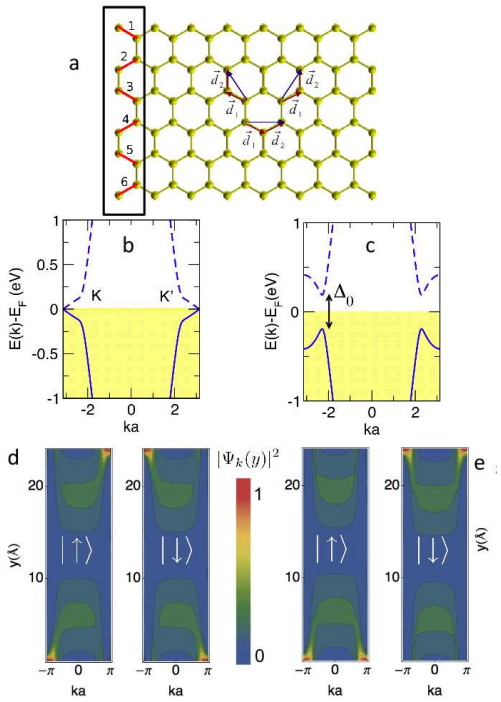

FIG. 1: (a) Honeycomb zigzag ribon with $N_y = 6$ atom rows. The second neighbour hopping vectors $\vec{d}_i$ are shown. (b) Low energy bands for the Spin Hall phase in $N_y = 12$ ribbon ($U = 0, t_{KM} = 0.01$ eV). (c) Low energy bands for the same ribbon with counter-polarized ferromagnetic edges ($U = 3$ eV and $t_{KM} = 0$). (d) Contour map of the valence band wave function $|\Psi_{k\sigma\nu}(y)|^2$ for spin up (left panel) and spin down (right panel). (e) Same than (d) for the magnetic ribbon.

that connect atom i and j with their common first neighbor (see figure 1a), $\hat{z}$ is the unit vector normal to the ribbon plane, and $\sigma = \pm 1$ indexes the spin projection along $\hat{z}$. For a flat ribbon, the SO term commutes with σ_z. The second term in eq. (1) describes Coulomb repulsion between electrons in the Hubbard approximation. We treat it in a mean field approximation so that we end up with an effective single particle Hamiltonian where the electrons interact with a spin dependent potential that is calculated self-consistently, $U \sum_i (n_{i,\uparrow}\langle n_{i,\downarrow}\rangle + n_{i,\downarrow}\langle n_{i,\uparrow}\rangle)$, so that σ_z is a good quantum number. Zigzag ribbons are defined by N_y, the number of zigzag chains which yield a total of $2N_y$ atoms per unit cell in a one dimensional crystal (fig. 1a). Importantly, the top and bottom edges belong to the two different triangular sub-lattices that define the honeycomb lattice. For a given wavenumber k and spin σ the mean field Hamiltonian has $2N_y$ states $\Psi_{k\sigma\nu}(y)$ with energy $\epsilon_{\sigma\nu}(k)$.

We consider first the model in the two limit cases, $U = 0, t_{KM} > 0$ and $t_{KM} = 0, U > 0$ for a ribbon with $N_Y = 12$. The highest occupied and lowest empty energy bands of the $U = 0, t_{KM} > 0$ case are shown in figure 1b. The special spin filtered edge states are the linear bands crossing the Fermi energy (E_F) The wave function squared, $|\Psi_{k,\sigma,\nu}(y)|^2$, of the valence band states are represented in figure 1d for $\sigma =\uparrow$ and $\sigma =\downarrow$ respectively. It is apparent that $\sigma =\uparrow$ ($\sigma =\downarrow$) electrons can only be in the top (bottom) edge for positive (negative) velocity states. Spin $\uparrow$ and $\downarrow$ electrons can also be in the bottom edge, but with velocity opposite to that of the top edge. Thus, the ribbon is conducting, the edges are not spin-polarized, but the states at the Fermi energy carry a net spin current. The electronic structure of the same ribbon, but now taking $t_{KM} = 0, U > 0$, is radically different. Instead of the linear spin-filtered bands there is a gap, Δ_0 so that the system is insulating. The wave-functions of the valence band are shown in figure 1e. They do not show correlation between spin and velocity, but they are edge-sensitive: top (bottom) edge is ferromagnetic with spin up (down) majority. The solution with reversed spins is equally valid.

In the light of figure 1, the question of how these competing electronic phases merge when both the Coulomb repulsion and the SO coupling are present calls for an answer. In figure 2 we show the energy bands for three cases, all with $U = t = 3$eV and $N_y = 12$. In the upper panels we show two cases with magnetic edges with total spin zero, one with with $t_{KM} = 0.01t$ and the second with $t_{KM} = 0.03t$. As shown in the inset, the magnetic moments are localized in the edges. In the small t_{KM} case, the system in an insulator, but the inter-edge gaps Δ_0 are now valley dependent. As the SO coupling increases the gap in one of the valleys closes completely, yet the edges are magnetic. This phase is radically different from the SO free case: a valley half-metal with magnetic edges antiferromagnetically oriented. In figure 2d we show how the magnetic moment in the edge atoms, $m = \frac{\langle n_\uparrow\rangle - \langle n_\downarrow\rangle}{2}$ is depleted as the strength of the spin orbit coupling is increased, reflecting the competition between the two terms in the Hamiltonian. Above a certain value of t_{KM}, the magnetic moment vanishes altogether and a Spin Hall insulator phase with conducting edge states identical to that with $U = 0$ is obtained. The calculated phase diagram in the (t_{KM}, U) plane showing the three different phases with zero total spin is shown in figure 3a, for the case of $N_Y = 12$. In figure 2c we show the conduction and valence band of the ferromagnetic phase with copolarized edges (see inset of fig. 2c). These bands preserve valley symmetry and intersect the Fermi energy, so that the edge states are conducting.

The evolution of the valley symmetry breaking, reflected by the different size of $\Delta_0(K)$ and $\Delta_0(K')$, is shown in figure 3b. The valley symmetry breaking can be understood using perturbative arguments. Close to the Dirac point the Kane-Mele Hamiltonian can be

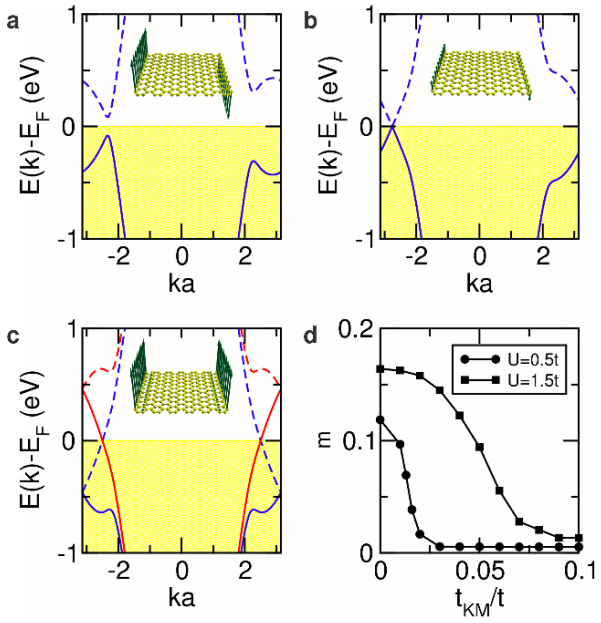

FIG. 2: (Color Online). Valence and conduction band of a $N_y = 12$ ribbon with $U = t = 3eV$ for three cases: (a) AF insulator with $t_{KM} = 0.01t$, (b), AF valley half metal $t_{KM} = 0.03t$ and (c) Co-polarized ferromagnetic edges $t_{KM} = 0.03t$. Insets:calculated magnetic density along the ribbon cell. (d) Depletion of the edge magnetic moment as the SO coupling t_{KM} is increased, for two different values of U/t.

approximated[3] by $V_{KM} = 3\sqrt{3}t_{KM}\sigma_z\tau_z\lambda_z$, where σ_z, τ_z and λ_z are the spin, valley and sub-lattice index respectively. Let us consider first the $(t_{KM} = 0, U > 0)$ antiferromagnetic phase (figure 1c,e) as starting point. The valence band is made of states with $\sigma_z =\uparrow$ and sublattice $\lambda_z = +$ (bottom edge) and states with $\sigma_z =\downarrow$ and sublattice $\lambda_z = -$ (upper edge), so that in both cases the product $\sigma_z\lambda_z$ has the same sign. Now it is apparent that the expectation value of $\sigma_z\tau_z\lambda_z$ has opposite signs in opposite valleys, so that in one case the gap opens and in the other closes, as shown in figure 2a.

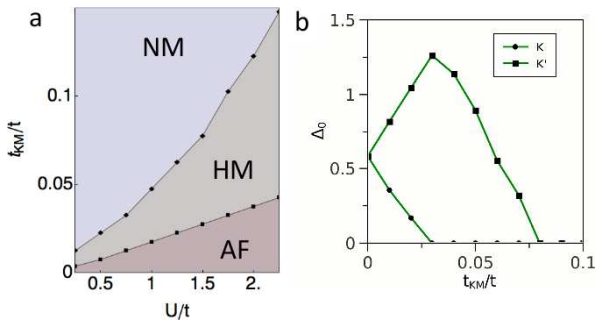

FIG. 3: (Color online). (a) Phase diagram for the AF insulating, AF valley half-metal (HM) and non-magnetic (NM) phases for the $N_y = 12$ ribbon. (b) Evolution of the gaps $\Delta_0(K)$ and $\Delta(K')$ as a function of the SO coupling.

In the non-interacting Kane-Mele model a non-equilibrium current I induces spin accumulation m in the edges[3]. This can be quantified as follows. We assume that a population of non-equilibrium extra electrons occupies the positive velocity states, so that the Fermi energy is increased by $\delta E_F = eV$. Using Landauer formula we have $I = 2\frac{e}{h}\delta E_F$, half of which goes on the top edge. From the non-interacting conduction band dispersion $\epsilon_k = \hbar v_F k$, we obtain δk_F and the corresponding change in density due to δE_F, $\delta n = \frac{\delta q}{a} = \frac{1}{\pi}\delta k_F$. Since δE_F is small, this extra density goes as spin $\uparrow$ to one edge and spin $\downarrow$ to the other. Thus, half of the extra charge goes to each edge fully spin-polarized, so that the edge magnetic moment reads $\delta m = \frac{1}{4}\delta q = \frac{1}{4\pi}\delta k_F a$. We can write the current in a given edge as

$$I_{edge} = 4\pi\frac{ev_F}{a}m \tag{2}$$

We now show that this picture survives in the interacting case in equilibrium. We find that in the ground state of the the magnetically ordered topological insulator phases shown in figure 2, charge currents flow on the edges, the total current accross a unit cell being null, in agreement with general theorems[26]. The current operator is given by the sum of link currents associated with all the sites b connected to a by single particle hopping:

$$\hat{I}_a = \frac{ei}{\hbar}\left(\sum_{b\sigma} t_{a,b}(\sigma)c^\dagger_{a,\sigma}c_{b,\sigma} - t_{b,a}(\sigma)c^\dagger_{b,\sigma}c_{a,\sigma}\right) \tag{3}$$

For a given eigenstate $\Psi_{k\sigma\nu}$ of the mean field Hamiltonian the current across the link ab reads

$$I_{ab}\left[\Psi\right] = 2\frac{e}{\hbar N}Im\left(\Psi^*_{k\sigma\nu}(b)\Psi_{k,\sigma,\nu}(a)t_{ab}(\sigma)e^{i\phi_{ab}}\right) \tag{4}$$

where $\phi_{ab} = 0$ for a and b in the same cell, $\phi_{ab} = \pm ka$ if a and b are in adjacent cells, and N is the number of cells in the crystal. The expectation value of this operator in the many-body ground state is obtained summing over all occupied bands: $\langle I_{ab}\rangle = \sum_{k,\nu,\sigma} f\left(\epsilon_{\nu\sigma}(k)\right) I_{ab}$. The average current is defined in the links of any pair of atoms connected by hopping in the one-body hamiltonian. In figure 4 we plot the ground state current map for the $N_y = 12$ ribbon for the AF insulating phase (fig 2a) and the ferromagnetic conducting phase (fig. 2c). The AF valley-half metal (not shown) is very similar to the AF insulator. The three electronic phases described in figure 2 present edge current of similar magnitude. Whereas in the FM case, currents flows in opposite directions in opposite edges, in the AF phases current runs parallel in the two edges. These results can be rationalized as if the magnetization plays the role of an external magnetic field. Thus, in the ferromagnetic case current flows is the same than in a Quantum Hall bar. In the antiferromagnetic phases, though, current flows parallel in the two edges, as if a magnetic field was pointing along opposite directions in the two edges.

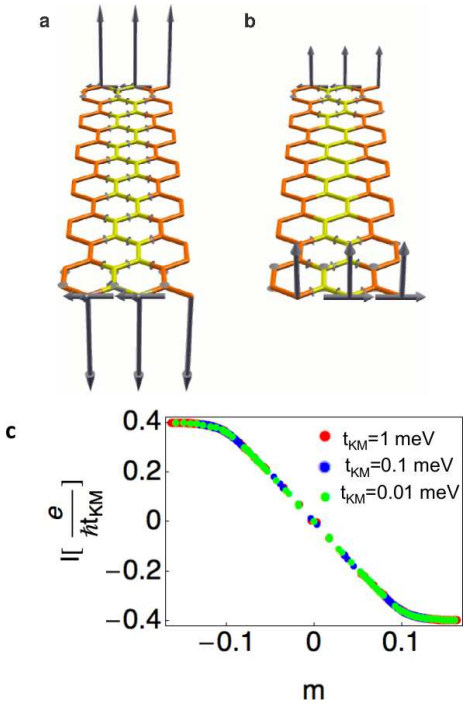

FIG. 4: Current and magnetization maps for (a) the AF insulating $N_y = 12$ ribbon and (b) the FM conducting one, both with $t_{KM} = 0.03t$ and $U = 1.0t$. The current between two atoms $\vec{r}_a$ and $\vec{r}_b$ is plotted as a vector along the line $\vec{r}_b - \vec{r}_a$, starting in the midpoint. (c), Edge charge current, in units of $\frac{e}{\hbar} t_{KM}$, as a function of the magnetic moment of the edge, for 3 values of $t_{KM} = 10^{-2}$, 10^{-1} and $1meV$, for the AF phases.

The magnitude of the top-edge current, normalized by $\frac{e}{\hbar} t_{KM}$, as a function of the top edge magnetization m collapses for several values of t_{KM} (figure 4c). For small m the curve is linear, $I_{edge} \simeq -4\frac{e}{\hbar} t_{KM} m$, in qualitative agreement with the analytical result of eq. (2), since $v_F = \gamma t_{KM} a/\hbar$ with $\gamma \simeq 6.5$. At larger m the edge current saturates to $|I_{edge}| \simeq 0.4\frac{e}{\hbar} t_{KM}$. If we take $t_{KM} = 10\mu eV$, close to the small values obtained by ab-initio calculations [27], we obtain an edge current of $\simeq 0.4nA$, well within reach of state of the art persistent current detection [28].

In conclusion, we propose a new mechanism for persistent charge currents. It involves the edge states of a two dimensional topological insulator with spontaneous ferromagnetic order induced by Coulomb interactions. We propose that this scenario occurs naturally in graphene zigzag ribbons. We find three new electronic phases in that system that combine ferromagnetic order and spontaneous charge current flow, both localized in the zigzag edges. They arise from the interplay of Coulomb repulsion and spin orbit coupling. When the ferromagnetic edges are counter-polarized, the valley symmetry is broken and, above a critical strength of the spin orbit coupling, the system goes from an insulating to a valley-half-metal phase. In the three phases, current flows as if there was a real magnetic field perpendicular to the sample along the direction of the magnetization edge. The question of weather our findings can be generalized to magnetically doped topological insulators will be addressed in future work.

This work has been financially supported by MEC-Spain (Grant Nos. MAT07-67845 and CONSOLIDER CSD2007-0010). We are indebted to J. J. Palacios, D. Gosalbez Martinez, C. Untiedt, F. Guinea, L. Brey and A. S. Nuñez, for fruitful discussions.

[1] P. W. Anderson, *Basic Notions of Condensed Matter Physics*, (Benjamin/Cummings, Menlo Park, CA, 1983).
[2] X. L. Qi, S. C. Zhang, Physics Today **63**, 33 (2010). M. Z. Hasan, C. L. Kane, arXiv:1002.3895 . J. E. Moore, Nature **464**, 194 (2010)
[3] C. L. Kane and E. J. Mele Phys. Rev. Lett. **95**, 226801 (2005)
[4] C. L. Kane and E. J. Mele Phys. Rev. Lett. **95**, 146802 (2005)
[5] B. A. Bernevig, T. L. Hughes and S. C. Zhang, Science **314**, 1757, (2006). X. L. Qi, Y. S. Wu and S. C. Zhang, Phys. Rev. B74, 085308, (2006), D. N. Sheng, Z. Y. Weng, L. Sheng, and F. D. M. Haldane Phys. Rev. Lett. **97**, 036808 (2006)
[6] N. A. Sinitsyn *et al.*, Phys. Rev. Lett. **97**, 106804 (2006)
[7] M. Konig, M. *et al.*, Science **318**, 766 (2007)
[8] Y. L. Chen *et al.* Science **325**, 178 (2009)
[9] K. Nakada, M. Fujita, G. Dresselhaus, and M. S. Dresselhaus, Phys. Rev. B **54**, 17954 (1996).
[10] M. Fujita, K. Wakabayashi, K. Nakada, and K. Kusakabe, J. Phys. Soc. Jpn. **65**, 1920 (1996).
[11] L. Brey, H. Fertig, Phys. Rev. B **73**, 235411 (2006)
[12] Y.-W. Son, M. L. Cohen, and S. G. Louie, Phys. Rev. Lett. **97**, 216803 (2006).
[13] Y.-W. Son, M. L. Cohen, and S. G. Louie, Nature **444**, 347 (2006).
[14] B. Ozyilmaz *et al.* Phys. Rev. Lett. **99**, 166804 (2007).
[15] A. H. Castro Neto, F. Guinea, N. M. R. Peres, K. S. Novoselov, A. K. Geim, Rev. Mod. Phys. **81**, 109 (2009)
[16] A. Rycerz, J. Tworzydo and C. W. J. Beenakker, Nature Physics **3**, 172 (2007)
[17] D. Gunlycke *et al.*,Nano Letters, **7**, 3608 (2007)
[18] O. V. Yazyev and M. I. Katsnelson, Phys. Rev. Lett. **100**, 047209 (2008).
[19] X. Li, X. Wang, L. Zhang, S. Lee, and H. Dai, Science **319**, 1229 (2008).
[20] J. Fernández-Rossier, Phys. Rev. B. **77**, 075430 (2008).
[21] W. Y. Kim and K. S. Kim, Nature Nanotechnology **3**, 408 (2008).
[22] F. Muñoz-Rojas, J. Fernández-Rossier, J. J. Palacios, Phys. Rev. Lett. **102**, 136810 (2009)
[23] H. Min et al., Phys. Rev. B **74**, 165310 (2006)
[24] Y. Yao, F. Ye, X. L. Qi, S. C. Zhang, Z. Fang, Phys. Rev. B**75**, 041401(R), (2007).
[25] F. D. M. Haldane, Phys. Rev. Lett. **61**, 2015 (1988)
[26] D. Bohm, Phys. Rev. **75**, 502 (1949)
[27] M. Gmitra *et al.*,Phys. Rev. B **80**, 235431 (2009)
[28] A. C. Bleszynski-Jayich *et al.*, Science **326**, 272 (2009)